Recent results on J/ψ and ψ(2S) production at ATLAS

Vakhtang Kartvelishvili

Lancaster University

(on behalf of the ATLAS Collaboration)

QwG Workshop, IISER Mohali, February 2024

Motivation

- Despite long history, hadronic production of quarkonium still poses many questions.
- Need to expand further the variety of experimental inputs to help theoretical understanding.
- Perturbative QCD have been reasonably successful in describing the non-prompt contributions, but a satisfactory understanding of the prompt production mechanisms is still to be achieved.
- It is hence increasingly important to broaden the scope of comparison between theory and experiment by providing a broader variety of experimental information on quarkonium production in a wider kinematic range.

This talk describes the methodology and results of the recent ATLAS measurement of the double-differential production cross sections of Prompt and Non-Prompt J/ψ and ψ(2S) production in pp collisions at 13 TeV **arXiv:2309:17177** **EPJC 84 (2024) 169**

Measurement strategy

ATLAS arXiv:2309:17177 EPJC 84 (2024) 169

Goal: measure the double-differential (in p_T and y) production cross-section of J/ψ and ψ(2S) mesons in pp collisions at 13 TeV, separately for prompt and non-prompt production mechanisms

- Channel: $\psi \rightarrow \mu^+\mu^-$
- Cover the widest possible range of transverse momentum for J/ψ and ψ(2S) by combining two triggers:

Low p_T range: $8 < p_T < 60$ GeV –

di-muon trigger "2mu4"

[2015 data, L=2.6/fb]

High p_T range: $60 < p_T < 360$ GeV –

single-muon trigger "mu50"

[full Run 2 data, L=140/fb]

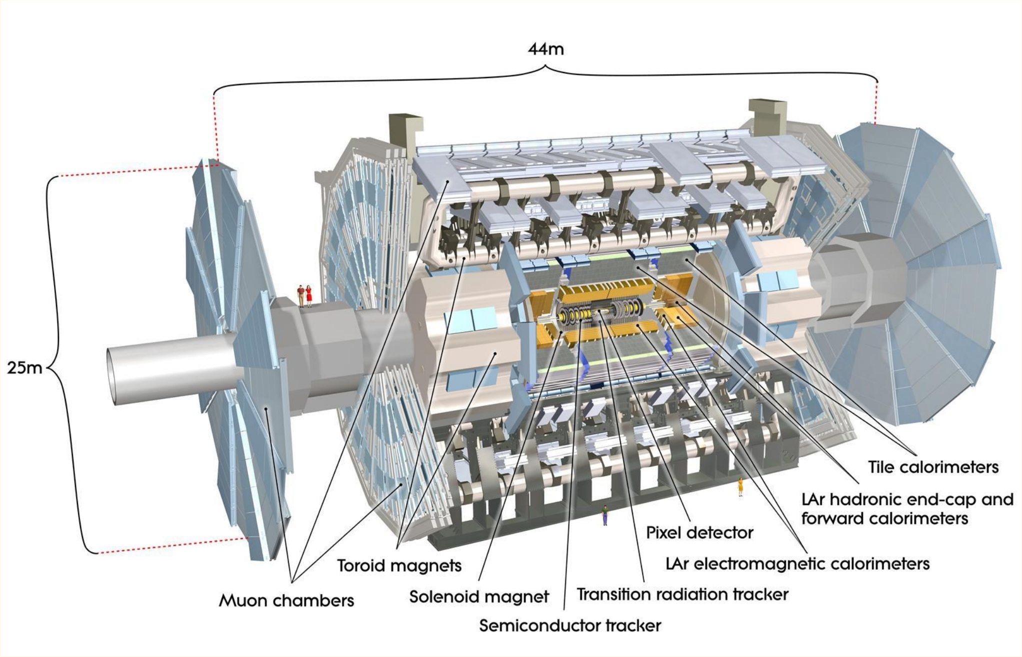

Measurement strategy - II

ψ = J/ψ or ψ(2S)

$$\frac{d^2\sigma^{P,NP}(pp \to \psi)}{dp_T dy} \times \mathcal{B}(\psi \to \mu^+\mu^-) = \frac{1}{\mathcal{A}(\psi)\epsilon_{\mathrm{trig}}\epsilon_{\mathrm{trigSF}}\epsilon_{\mathrm{reco}}\epsilon_{\mathrm{recoSF}}} \frac{N_\psi^{P,NP}}{\Delta p_T \, \Delta y \, \int \mathcal{L} dt}$$

- A(ψ) - the geometrical acceptance calculated separately for low p T and high p T bins, using the cuts:
  - in low p_T range: p_T (μ1) > 4 GeV, p_T (μ2) > 4 GeV, $|\eta(\mu 1), \eta(\mu 2)| < 2.4$
  - in high p_T range: p_T (μ1) > 52.5 GeV, p_T (μ2) > 4 GeV, $|\eta(\mu 1), \eta(\mu 2)| < 2.4$
- ϵ_{trig} - the trigger efficiency, calculated using MC Monte Carlo samples.
- $\epsilon_{\mathrm{trigSF}}$ - the trigger correction scale factor accounting for MC-data differences.
- ϵ_{reco} - the reconstruction efficiency, calculated using the Monte Carlo samples.
- $\epsilon_{\mathrm{recoSF}}$ - the reconstruction efficiency correction scale factor accounting for MC-data differences.
- **$N_\psi^{P,NP}$ - the raw yields of J/ψ and ψ(2S), obtained from 2D maximum likelihood fits.**
- Δp_T and Δy - corresponding bin widths in p_T and absolute rapidity.
- $\int L dt$ - the corresponding integrated luminosity.

The fit model

2D unbinned maximum likelihood fit is done to obtain raw yields - $N_{\psi}^{P,NP}$

$$PDF(m,\tau) = \sum_{i=1}^{7} \kappa_i f_i(m) \cdot (h_i(\tau) \otimes R(\tau)) \cdot C_i(m,\tau).$$

Prompt ψ candidates are distinguished from those originating from b-hadron decays through the separation L_{xy} of the primary vertex and the ψ decay vertex.

i	Type	P/NP	$f_i(m)$	$h_i(\tau)$
1	J/ψ	P	$\omega_0 G_1(m) + (1-\omega_0)[\omega_1 CB(m) + (1-\omega_1)G_2(m)]$	$\delta(\tau)$
2	J/ψ	NP	$\omega_0 G_1(m) + (1-\omega_0)[\omega_1 CB(m) + (1-\omega_1)G_2(m)]$	$\omega_2 E_1(\tau) + (1-\omega_2)E_1(b\tau)$
3	$\psi(2S)$	P	$\omega_0 G_1(\beta m) + (1-\omega_0)[\omega_1 CB(\beta m) + (1-\omega_1)G_2(\beta m)]$	$\delta(\tau)$
4	$\psi(2S)$	NP	$\omega_0 G_1(\beta m) + (1-\omega_0)[\omega_1 CB(\beta m) + (1-\omega_1)G_2(\beta m)]$	$E_2(\tau)$
5	Bkg	P	P	$\delta(\tau)$
6	Bkg	NP	$E_3(m)$	$E_4(\tau)$
7	Bkg	NP	$E_5(m)$	$E_6(\|\tau\|)$

The pseudo-proper time:

$$\tau = \frac{m_{\mu\mu}}{p_{\mathrm{T}}} \frac{L_{xy}}{c}$$

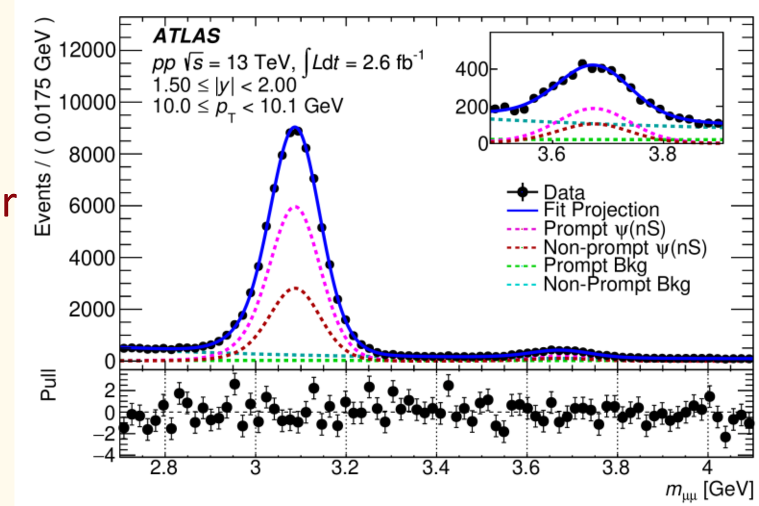

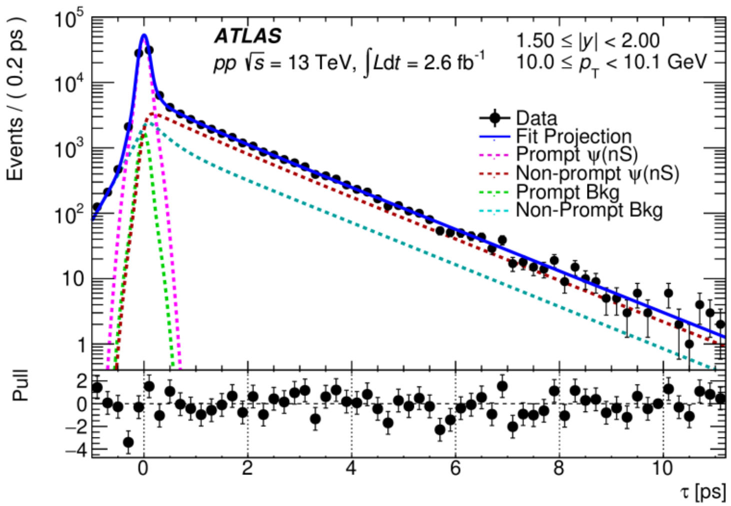

More fit examples

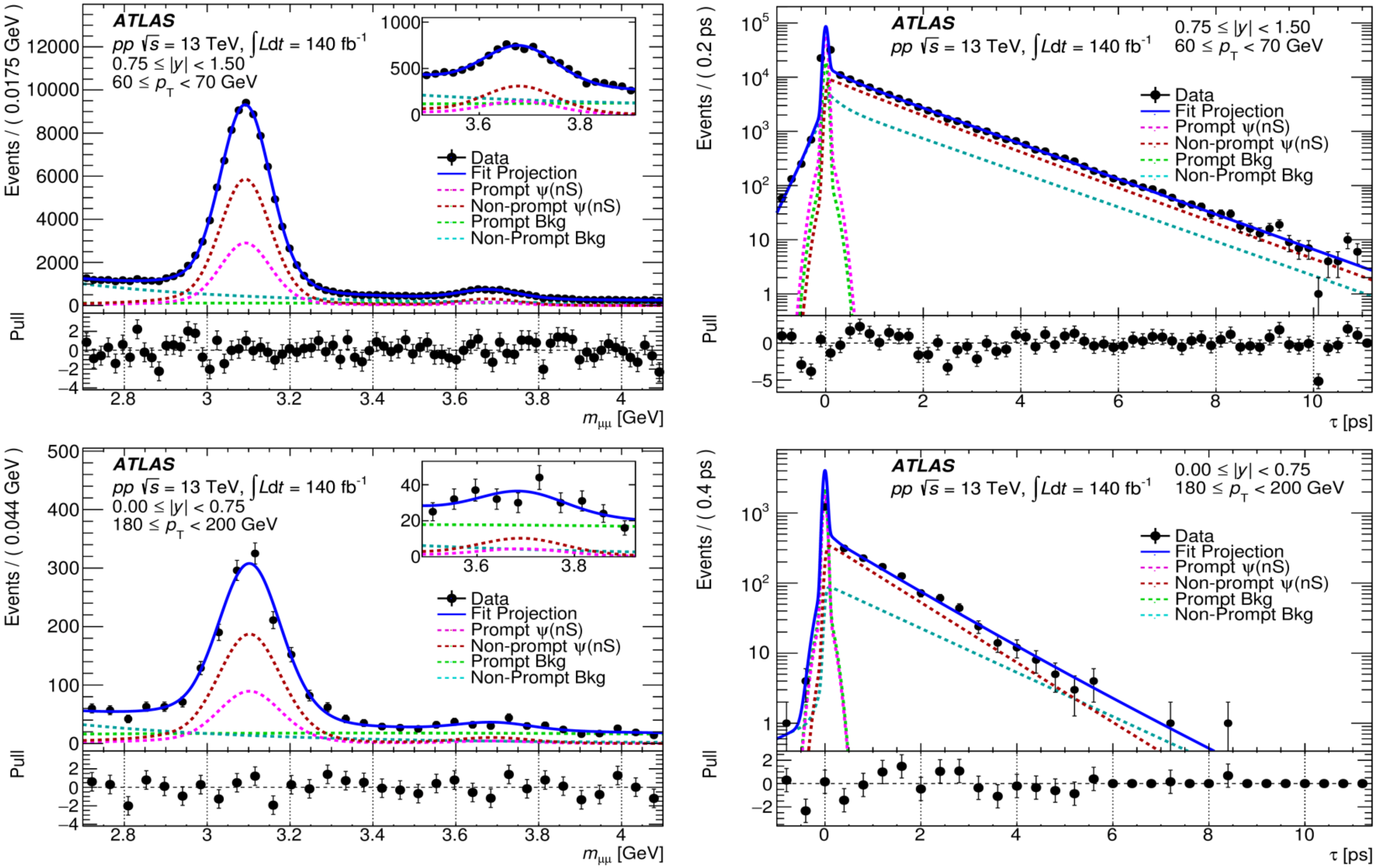

The same fit model is used throughout the full kinematic range.
Pull distributions and 2D χ^2 values are used to assess fit quality.

Systematics

Sources of systematic uncertainties:

1. **Acceptance systematics.**
2. **Trigger efficiency systematics**
3. **Reconstruction efficiency systematics**
4. **Fit model systematics.**
5. **Luminosity uncertainty.**
6. **Spin alignment correction factors.**

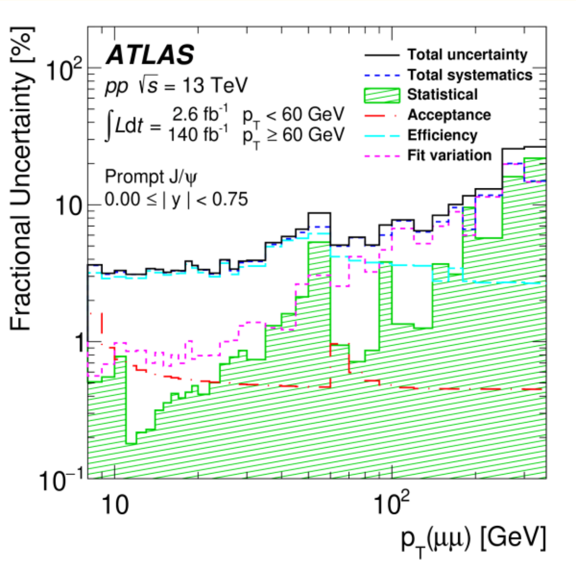

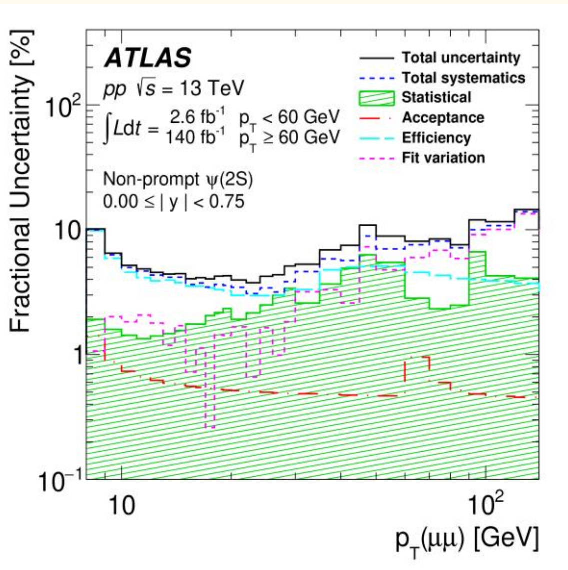

Structures visible on the plots:

- **binning changes**
- **statistical effects**
- **change of trigger**

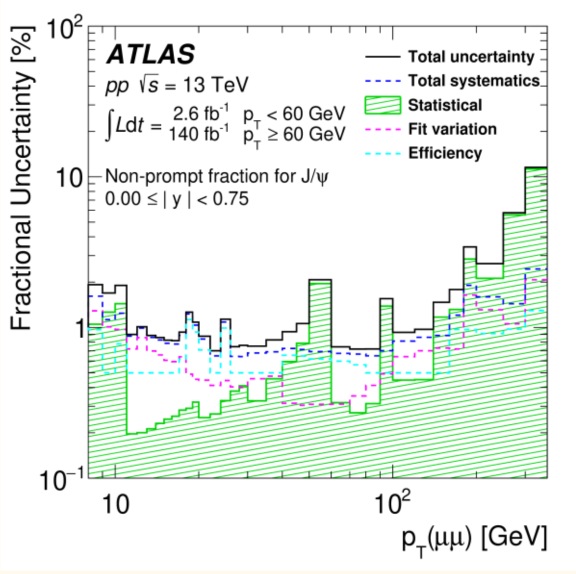

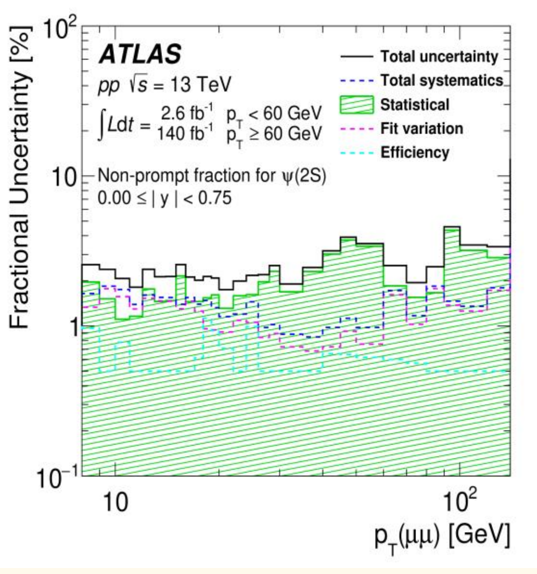

Results: 1 - J/ψ differential cross sections

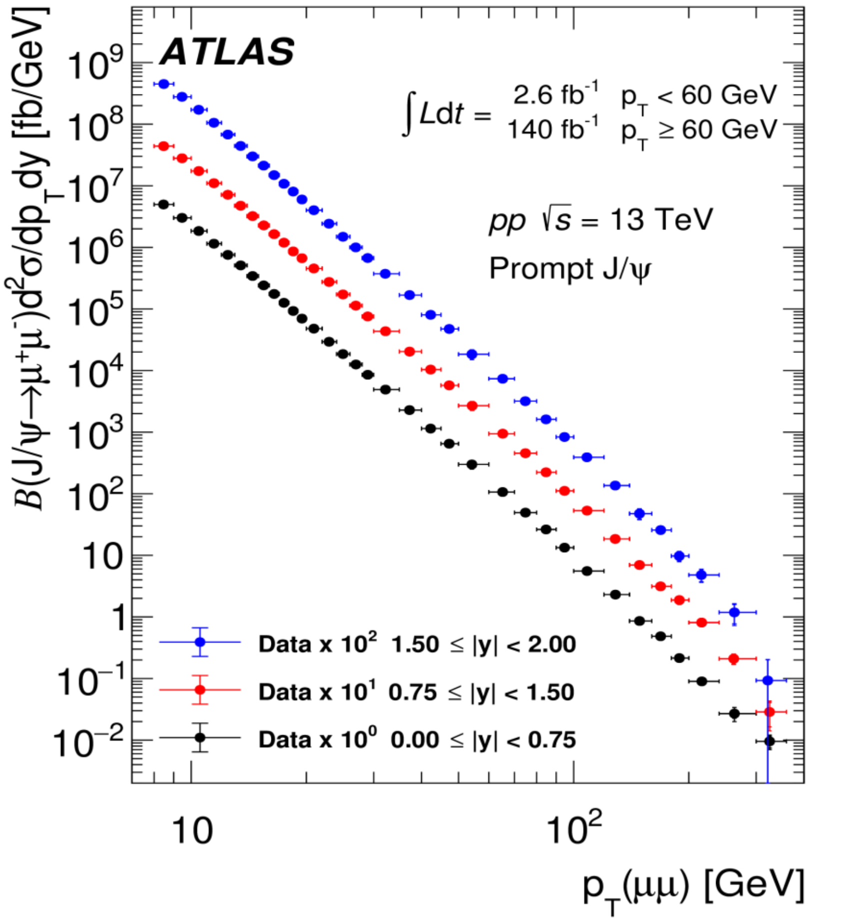

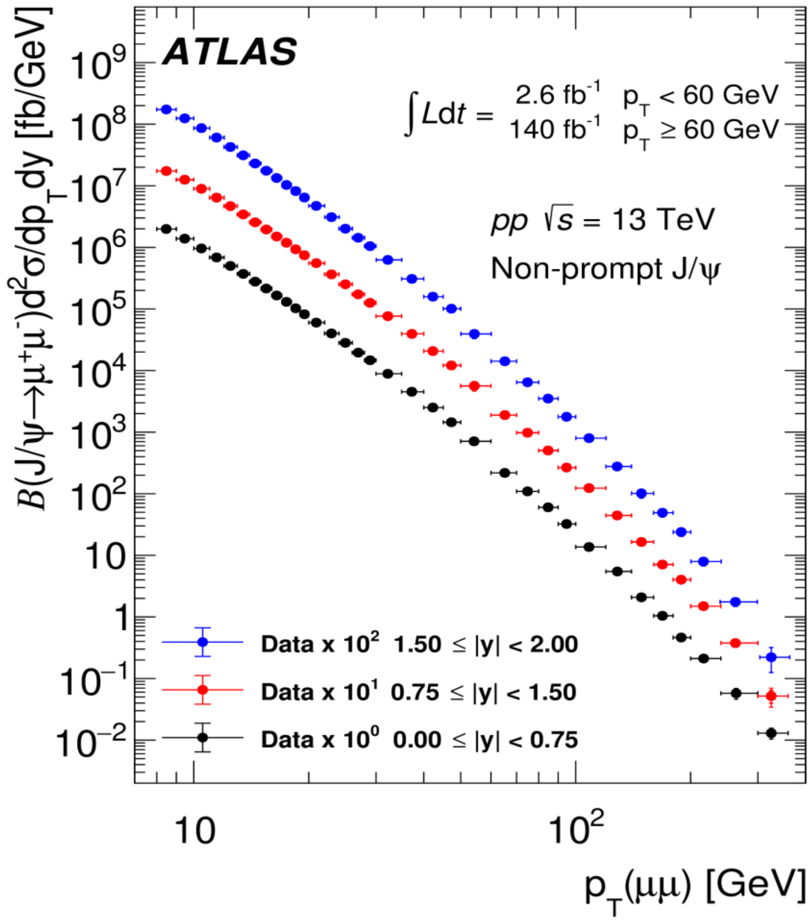

- **Three rapidity ranges shifted for visual clarity**
- **Widest pT range achieved so far: 8 GeV to 360 GeV**
- **Almost 9 orders of magnitude variation of cross section**

Measurement comparison, central *y*

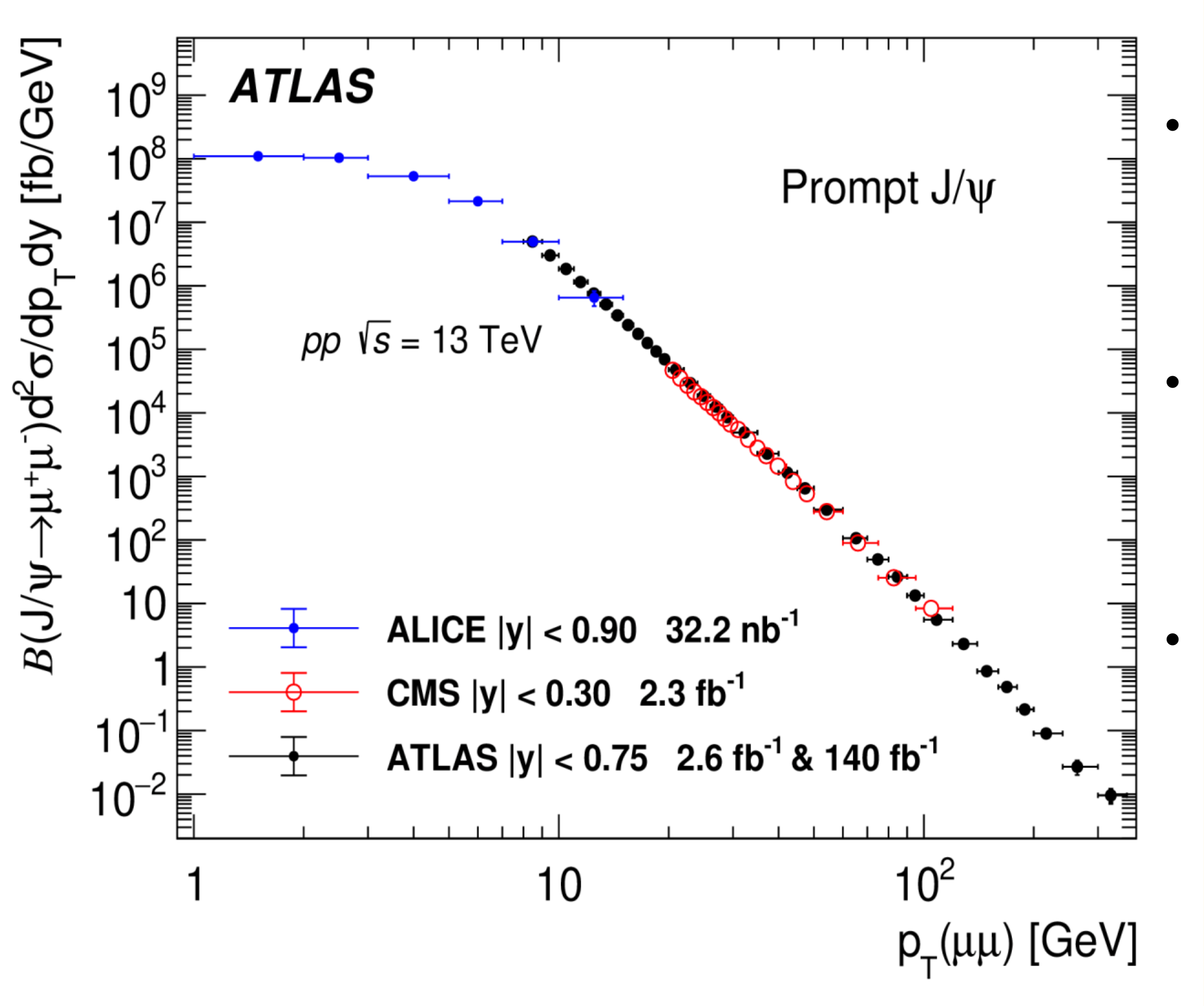

- ALICE [1 – 15] GeV]
  JHEP 03 (2022) 190
- CMS [20 – 120] GeV
  Phys. Lett. B 780 (2018) 251
- ATLAS [8 – 360] GeV
  arXiv:2309:17177
  EPJC 84 (2024) 169

Results: 2 - ψ(2S) differential cross sections

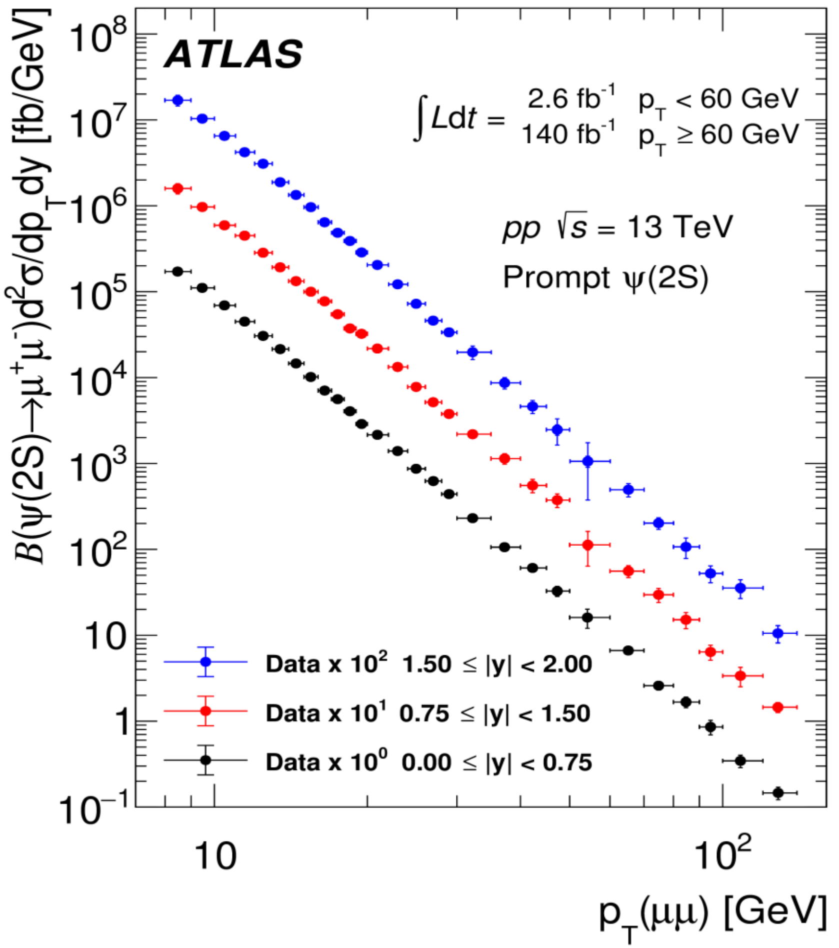

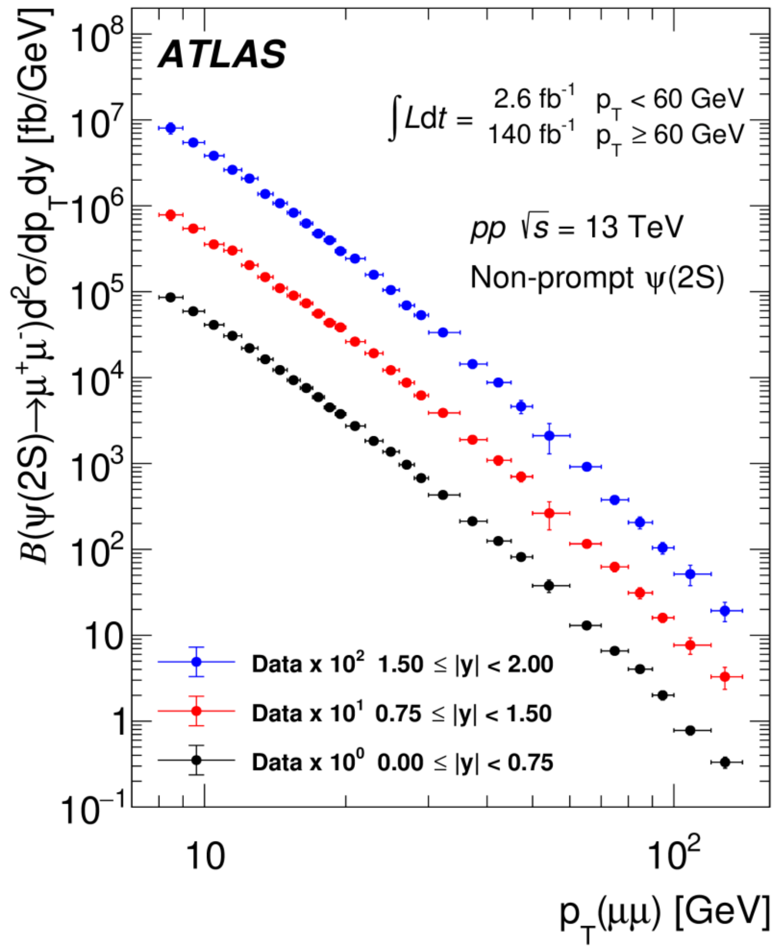

- **Three rapidity ranges shifted for visual clarity**
- **Widest pT range so far: 8 GeV to 140 GeV**
- **More than 6 orders of magnitude variation of cross section**

Results: 3 - ψ(2S)-to-J/ψ production ratios

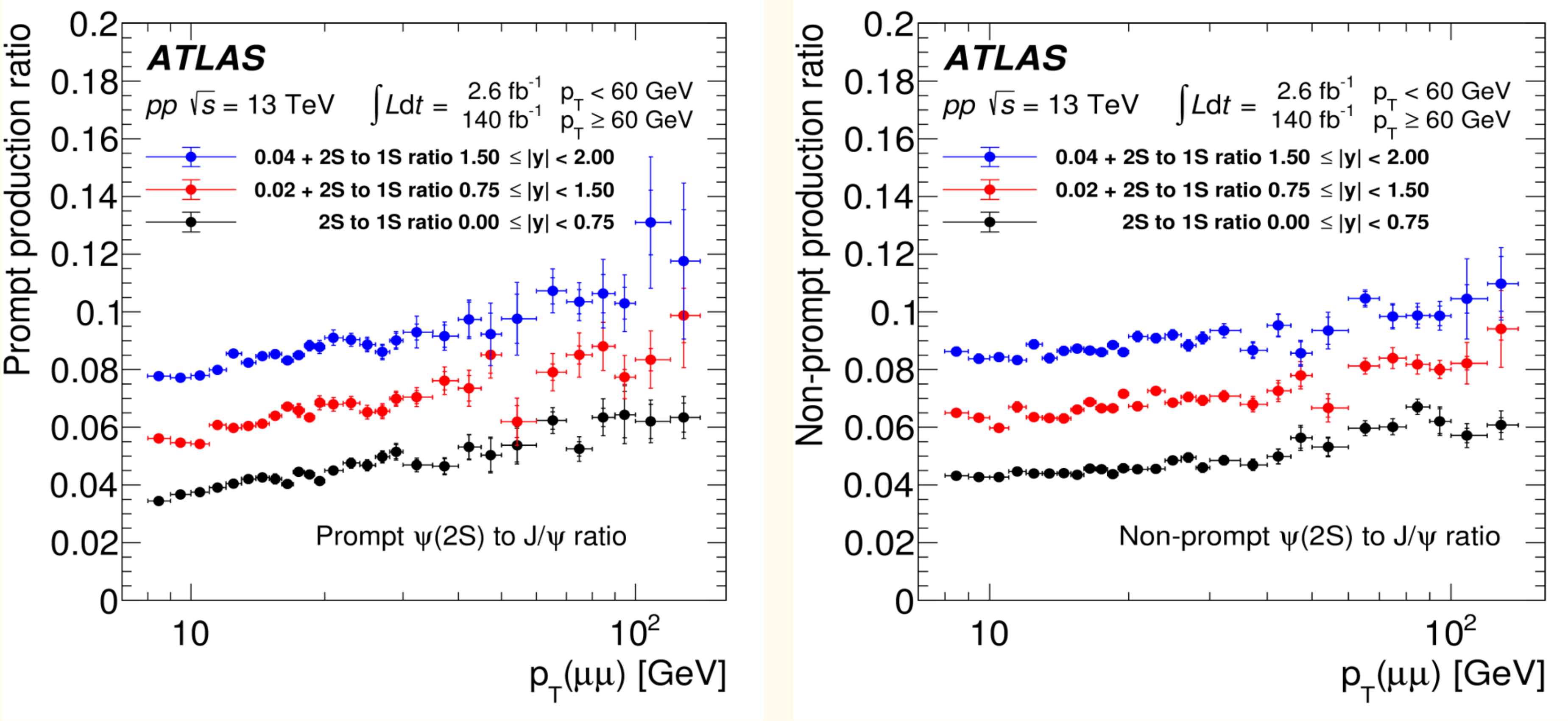

- **Three rapidity ranges shifted for visual clarity**
- **Seem independent of rapidity**
- **Prompt ratio increases faster with pT**

Results: 4 – Non-prompt fractions

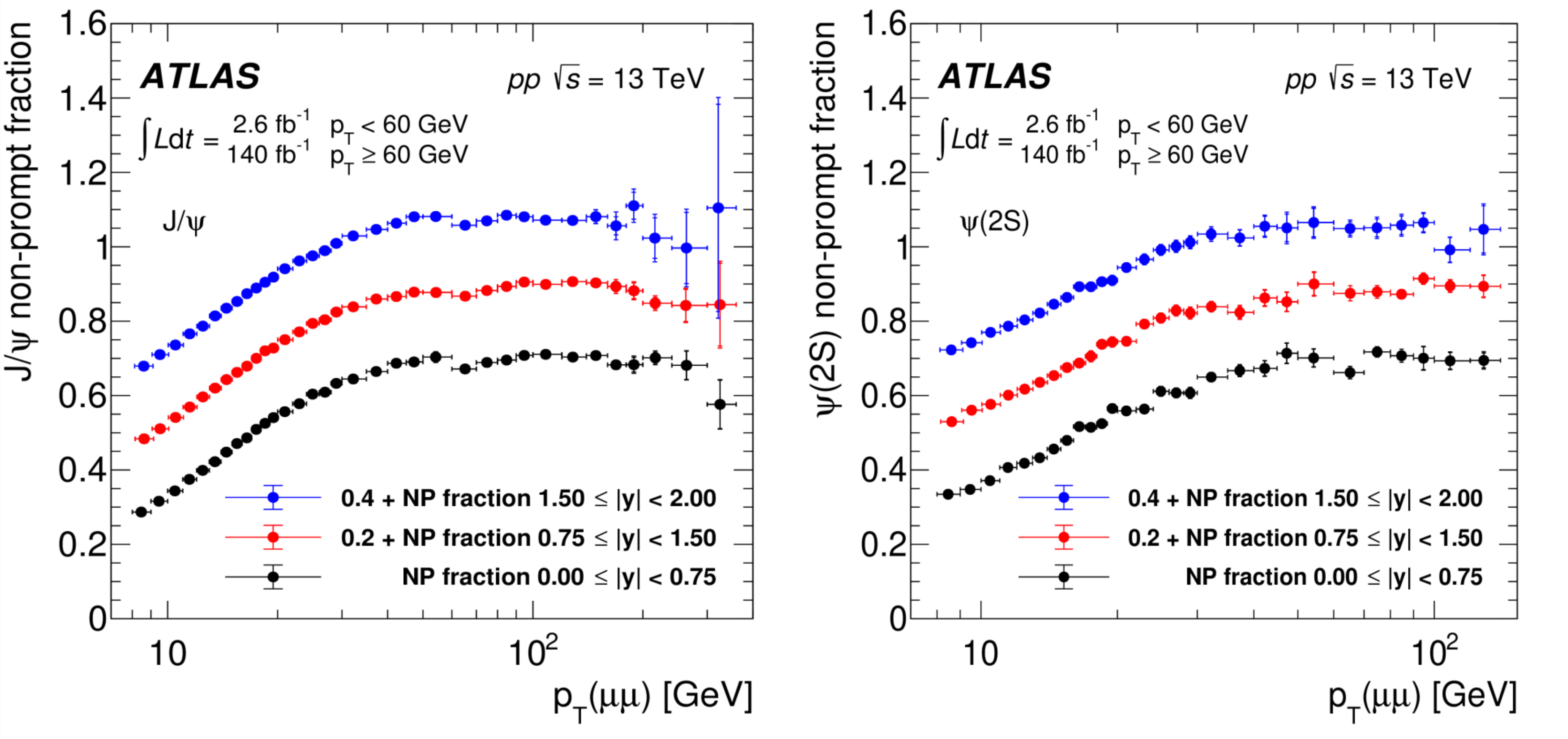

- Three rapidity ranges shifted for visual clarity
- Fast increase at low pT, stabilise after 50 GeV
- Similar behaviour for J/ψ and ψ(2S)
- Step at 60 GeV (trigger change) – Spin alignment to blame?

Spin alignment corrections for Acceptance

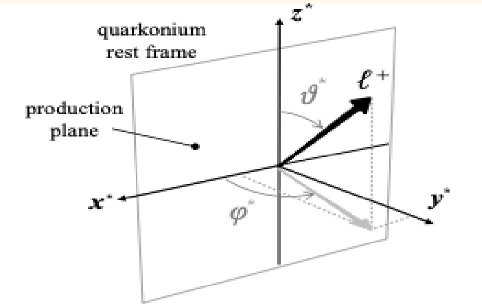

Figure from P. Faccioli

General angular dependence for ψ → mu⁺mu⁻ decay:

$$\frac{d^2N}{d\cos\theta^\star d\phi^\star} \propto 1 + \lambda_\theta \cos^2\theta^\star + \lambda_\phi \sin^2\theta^\star \cos 2\phi^\star + \lambda_{\theta\phi} \sin 2\theta^\star \cos\phi^\star$$

Coefficients λ_θ , λ_ϕ and $\lambda_{\theta\phi}$ are related to the spin-density matrix elements of the dimuon spin wave function for various polarisations.

- **Dependence of acceptance on λ_ϕ and $\lambda_{\theta\phi}$ is weak, but λ_θ can be significant.**
- **Nominal analysis assumes isotropic production, all $\lambda = 0$.**
- **Correction factors shown for λ_θ = +/- 0.2, reflecting the level of experimental knowledge**
- **Could be different for prompt and non-prompt production, step at 60 GeV**

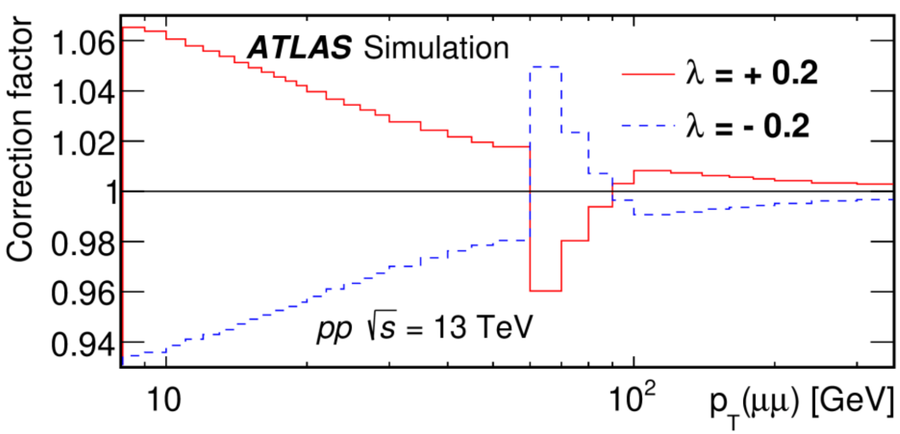

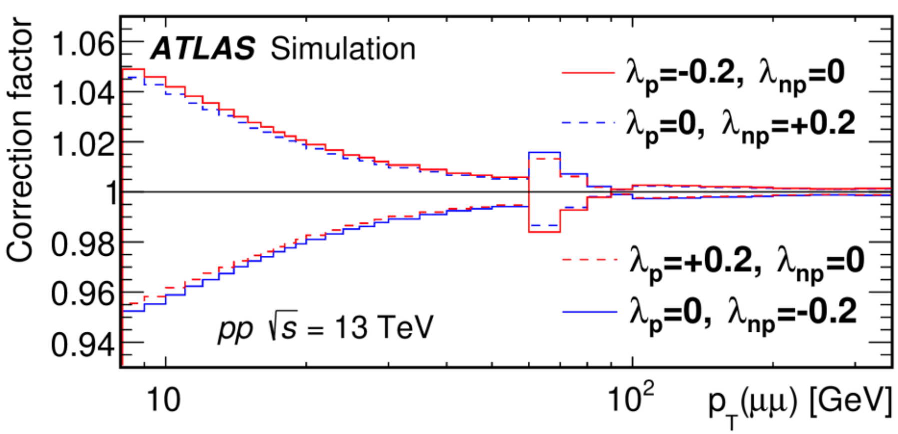

Theory comparison: prompt J/ψ and ψ(2S)

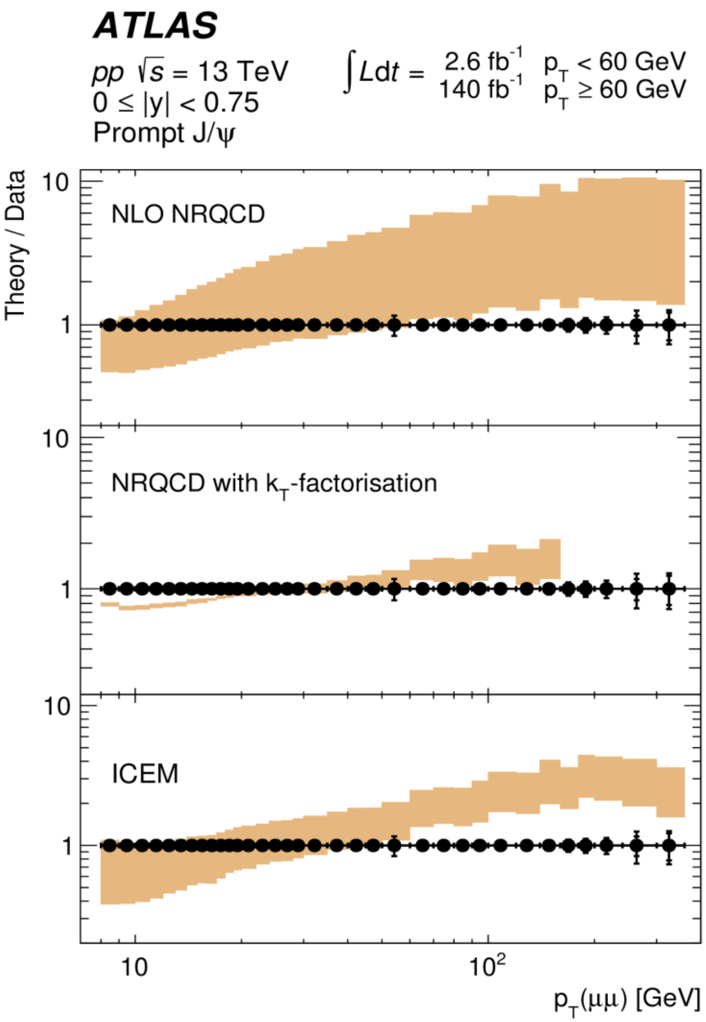

ATLAS

EPJC84(2024)169

arXiv:2309:17177

Butenschön,Kniehl [1-3]

Baranov et al [4-7]

Cheung,Vogt [8]

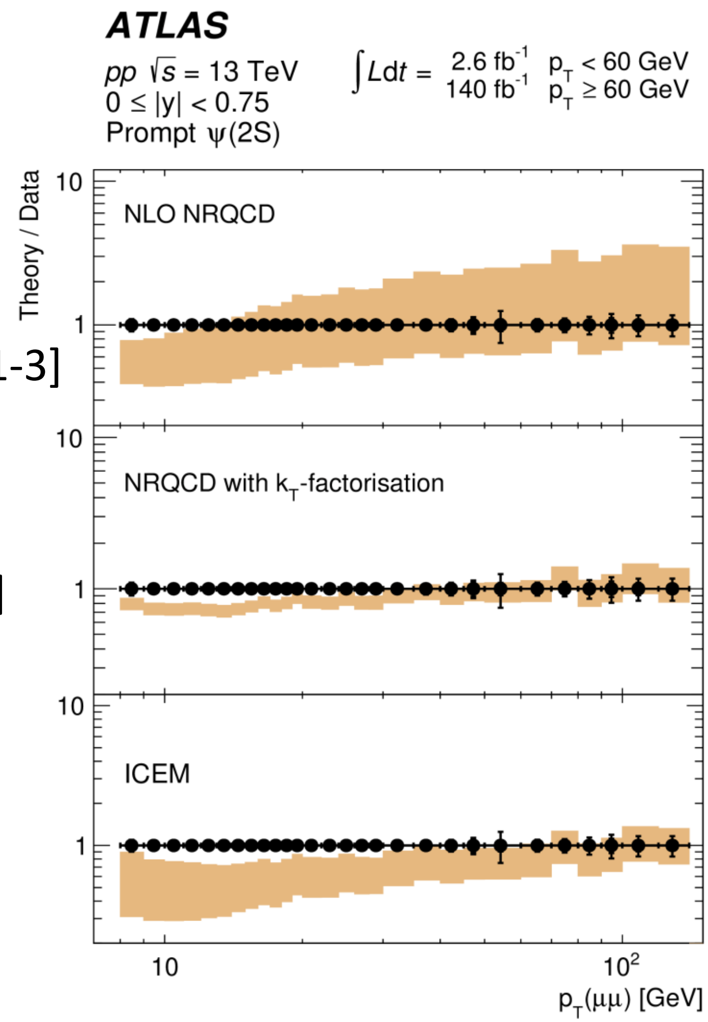

9 orders of magnitude described within a factor of ~3

There is room for improvement for all models shown

Theory comparison: non-prompt J/ψ and ψ(2S)

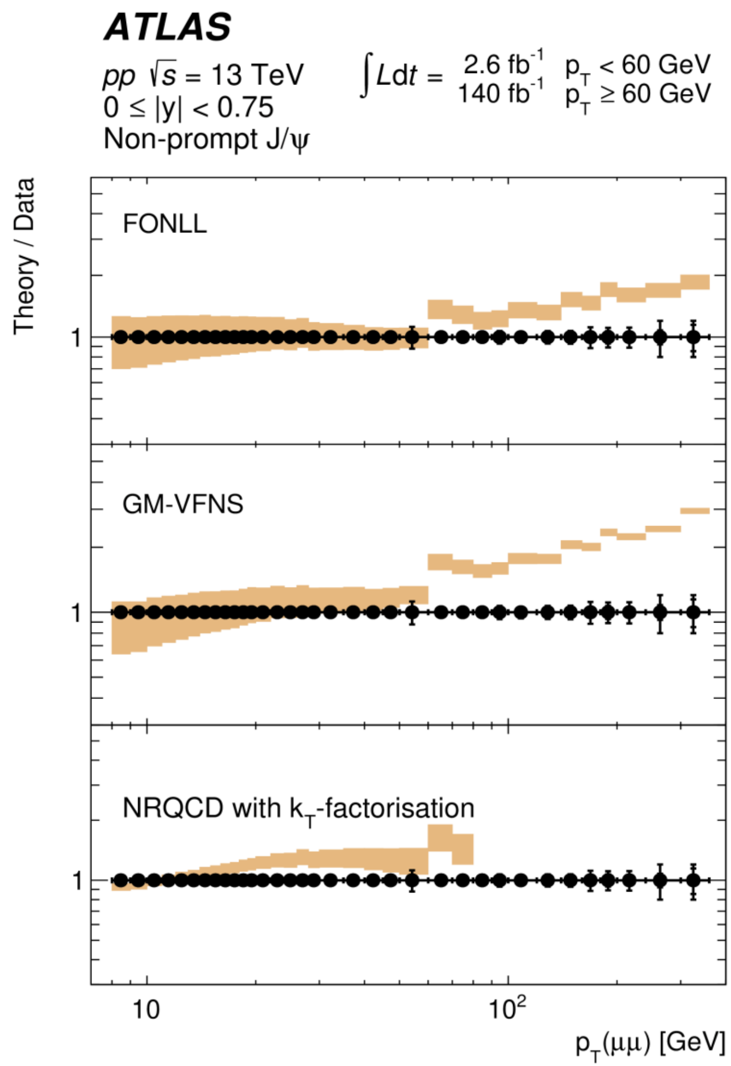

ATLAS

EPJC84(2024)169

arXiv:2309:17177

Cacciari et al [9-11]

Kniehl et al [12-14]

Baranov et al [6,15]

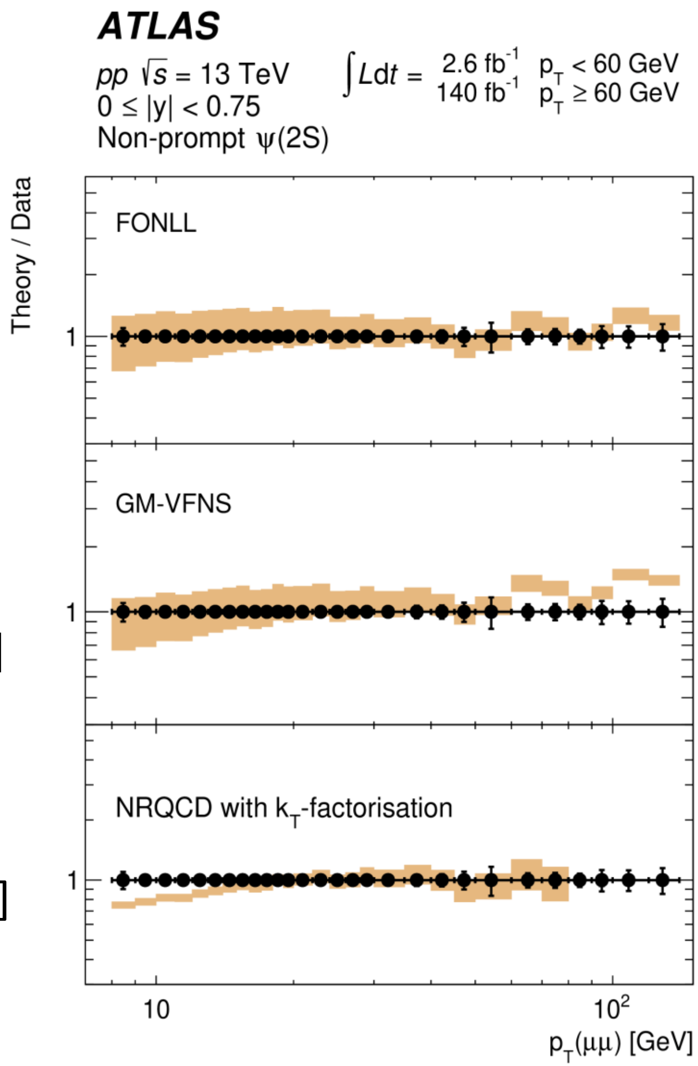

Generally better agreement for non-prompt, still tend to overestimate at high pT

Summary

Explained the procedure and the results of a measurement of J/ψ and $\psi(2S)$ production, using the ATLAS detector and the full Run 2 data set collected with pp collisions at 13 TeV.

Measured distributions:

- Double-differential cross-sections for prompt J/ψ and $\psi(2S)$;
- Double-differential cross-sections for non-prompt J/ψ and $\psi(2S)$;
- Non-prompt fractions of J/ψ and $\psi(2S)$;
- production ratios of $\psi(2S)$ to J/ψ.

ATLAS
EPJC84(2024)169
arXiv:2309:17177

Covered rapidity range between −2 and +2 in three bins;

Covered transverse momentum range well beyond previously achieved

- for J/ψ : 8 to 360 GeV;
- for $\psi(2S)$: 8 to 140 GeV.

ATLAS results are consistent with similar results from CMS and ALICE collaborations.

A variety of theoretical predictions for both Prompt and Non-prompt production were compared to the ATLAS results - they describe the data with varying levels of success.

For your convenience, all data points from this measurement are available on HEPDATA.

References for theoretical models

[1] M. Butenschön and B. A. Kniehl, Reconciling J/ψ Production at HERA, RHIC, Tevatron, and LHC with Nonrelativistic QCD Factorization at Next-to-Leading Order, Phys. Rev. Lett. 106 (2011) 022003.
[2] M. Butenschoen and B. A. Kniehl, World data of J/ψ production consolidate nonrelativistic QCD factorization at next-to-leading order, Phys. Rev. D 84 (2011) 051501.
[3] M. Butenschoen and B. A. Kniehl, Global analysis of ψ(2S) inclusive hadroproduction at next-to-leading order in nonrelativistic-QCD factorization, Phys. Rev. D 107 (2023) 034003, arXiv: 2207.09346.
[4] S. P. Baranov, A. V. Lipatov and N. P. Zotov, Prompt charmonia production and polarization at LHC in the NRQCD with kT -factorization. Part I: $\psi(2S)$ meson, Eur. Phys. J. C 75 (2015) 455, arXiv: 1508.05480 [hep-ph].
[5] S. P. Baranov and A. V. Lipatov, Prompt charmonia production and polarization at the LHC in the NRQCD with kT-factorization. III. J/ψ meson, Phys. Rev. D 96 (2017) 034019.
[6] A. V. Lipatov, M. A. Malyshev and S. P. Baranov, Particle Event Generator: A Simple-in-Use System PEGASUS version 1.0, Eur. Phys. J. C 80 (2020) 330, arXiv: 1912.04204 [hep-ph].
[7] S. P. Baranov and A. V. Lipatov, Are there any challenges in the charmonia production and polarization at the LHC?, Phys. Rev. D 100 (2019) 114021.
[8] V. Cheung and R. Vogt, Production and polarization of direct J/ψ to O (α 3 s) in the improved color evaporation model in collinear factorization, Phys. Rev. D 104 (2021) 094026.
[9] M. Cacciari, S. Frixione and P. Nason, The pT spectrum in heavy flavor photoproduction, JHEP 03 (2001) 006, arXiv: hep-ph/0102134. 21
[10] M. Cacciari et al., Theoretical predictions for charm and bottom production at the LHC, JHEP 10 (2012) 137, arXiv: 1205.6344 [hep-ph].
[11] M. Cacciari, FONLL Heavy Quark Production, http://www.lpthe.jussieu.fr/~cacciari/fonll/fonllform.html, Accessed: 2019-09-03.
[12] P. Bolzoni, B. A. Kniehl and G. Kramer, Inclusive J/ψ and $\psi(2S)$ production from b-hadron decay in pp and $p\ p$ collisions, Phys. Rev. D 88 (2013) 074035.
[13] B. A. Kniehl, G. Kramer, I. Schienbein and H. Spiesberger, Cross sections of inclusive $\psi(2S)$ and $X(3872)$ production from b-hadron decays in $p\ p$ collisions and comparison with ATLAS, CMS, and LHCb data, Phys. Rev. D 103 (2021) 094002.
[14] M. Butenschoen and B. A. Kniehl, World data of J/ψ production consolidate nonrelativistic QCD factorization at next-to-leading order, Phys. Rev. D 84 (2011) 051501.
[15] S. P. Baranov, A. V. Lipatov and M. A. Malyshev, Associated non-prompt J/ψ + μ and J/ψ + J/ψ production at LHC as a test for TMD gluon density, Eur. Phys. J. C 78 (2018) 820, arXiv: 1808.06233.

THANK YOU!

ATLAS data vs Butenschoen, Kniehl

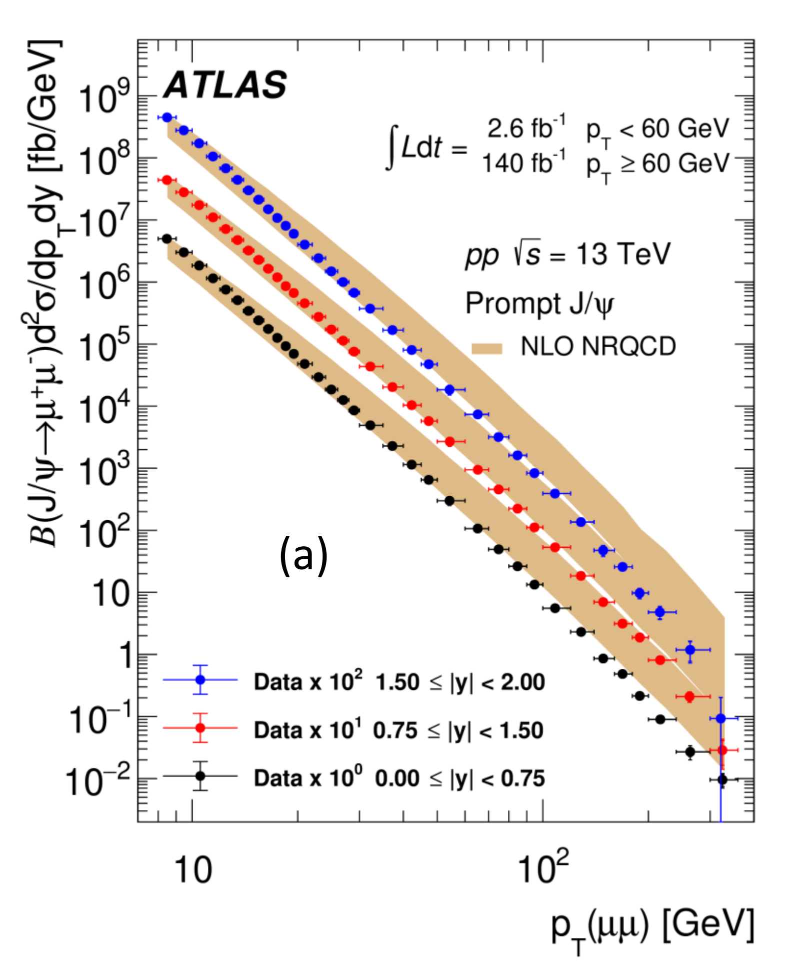

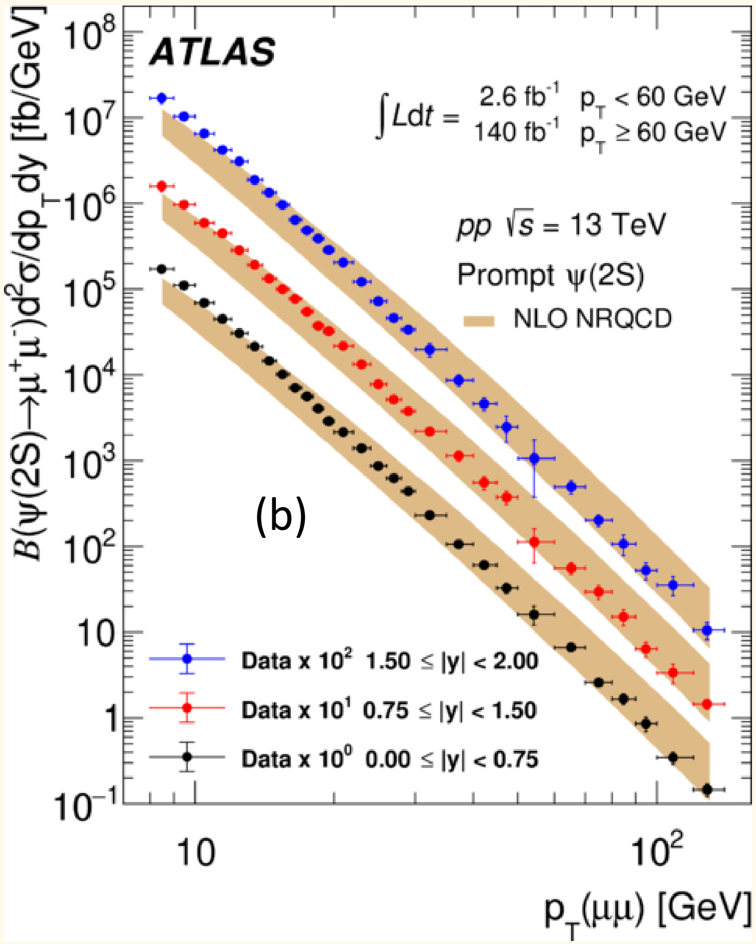

ATLAS arXiv:2309.17177 EPJC84(2024)169

Differential cross sections of (a) prompt J/ψ and (b) prompt ψ(2S) overlaid with the predictions of NLO NRQCD model [1] with LDMEs pre-determined in [2,3]. Model uncertainties include variations of renormalisation, factorisation and NRQCD scales.

ATLAS data vs Baranov et al.

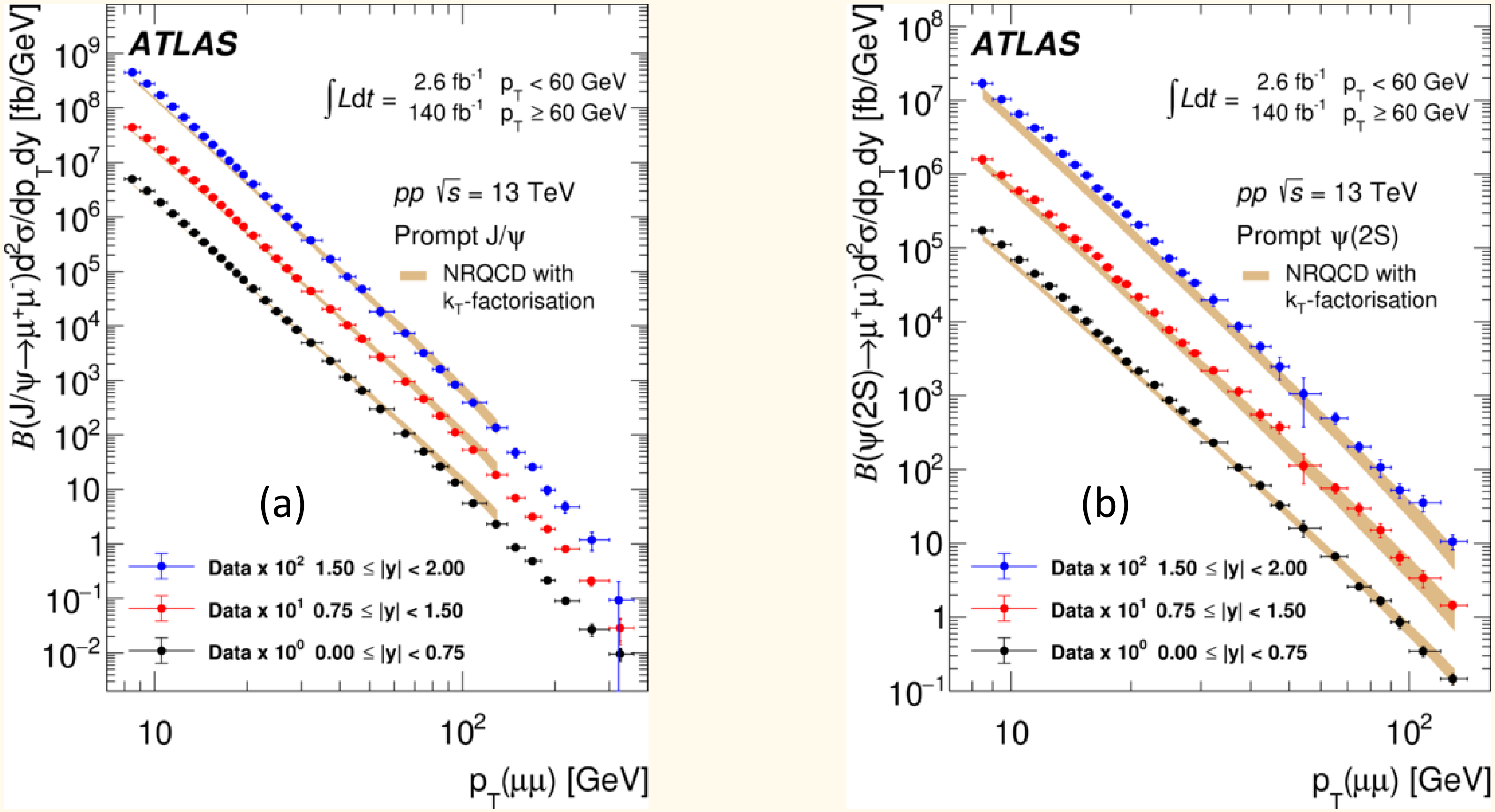

ATLAS arXiv:2309:17177 EPJC84(2024)169

Differential cross sections of prompt J/ψ (a) and prompt ψ(2S) (b) overlaid with predictions from the k_T-factorisation model [4,5], obtained with the PEGASUS event generator [6] using the LDMEs determined in Ref. [7]. Theoretical uncertainties are due to variation in the renormalisation scale alone. The range of comparison is limited by the availability of the transverse-momentum-dependent gluon PDF.

ATLAS data vs Cheung, Vogt

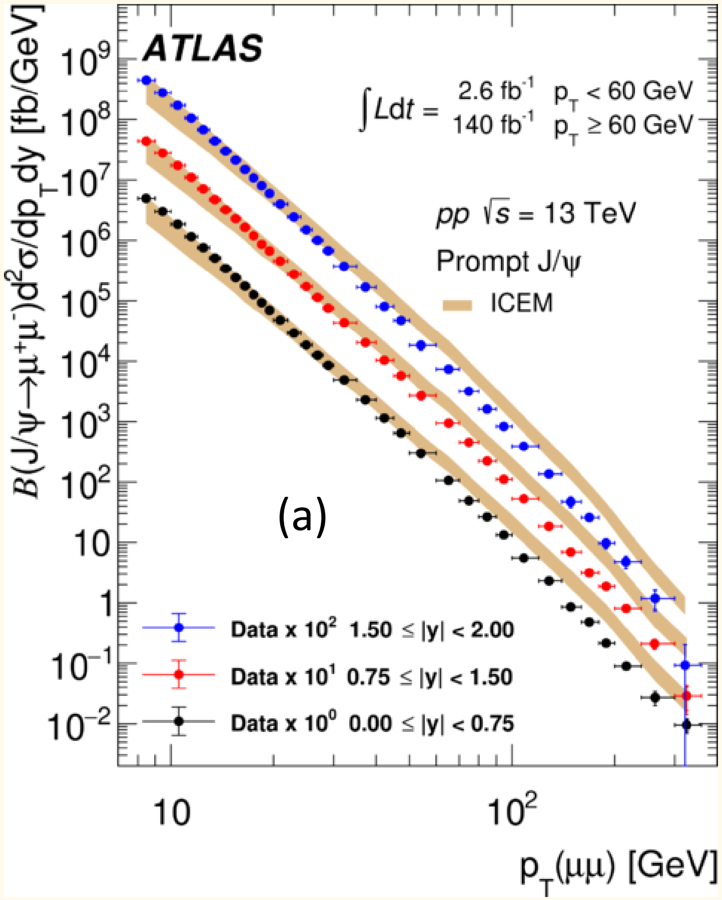

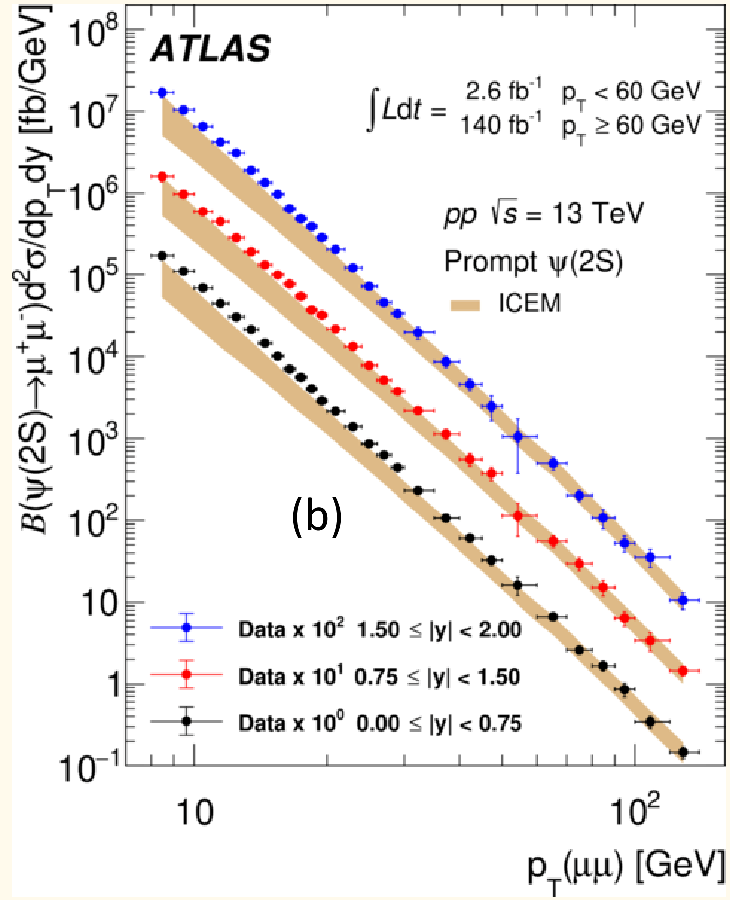

ATLAS arXiv:2309.17177 EPJC84(2024)169

Differential cross sections of (a) prompt J/ψ and (b) prompt ψ(2S), overlaid with predictions of the Improved Colour Evaporation Model [8], with parameters and their uncertainties previously determined from fits to LHCb data at 7 TeV.

ATLAS data vs Cacciari et al.

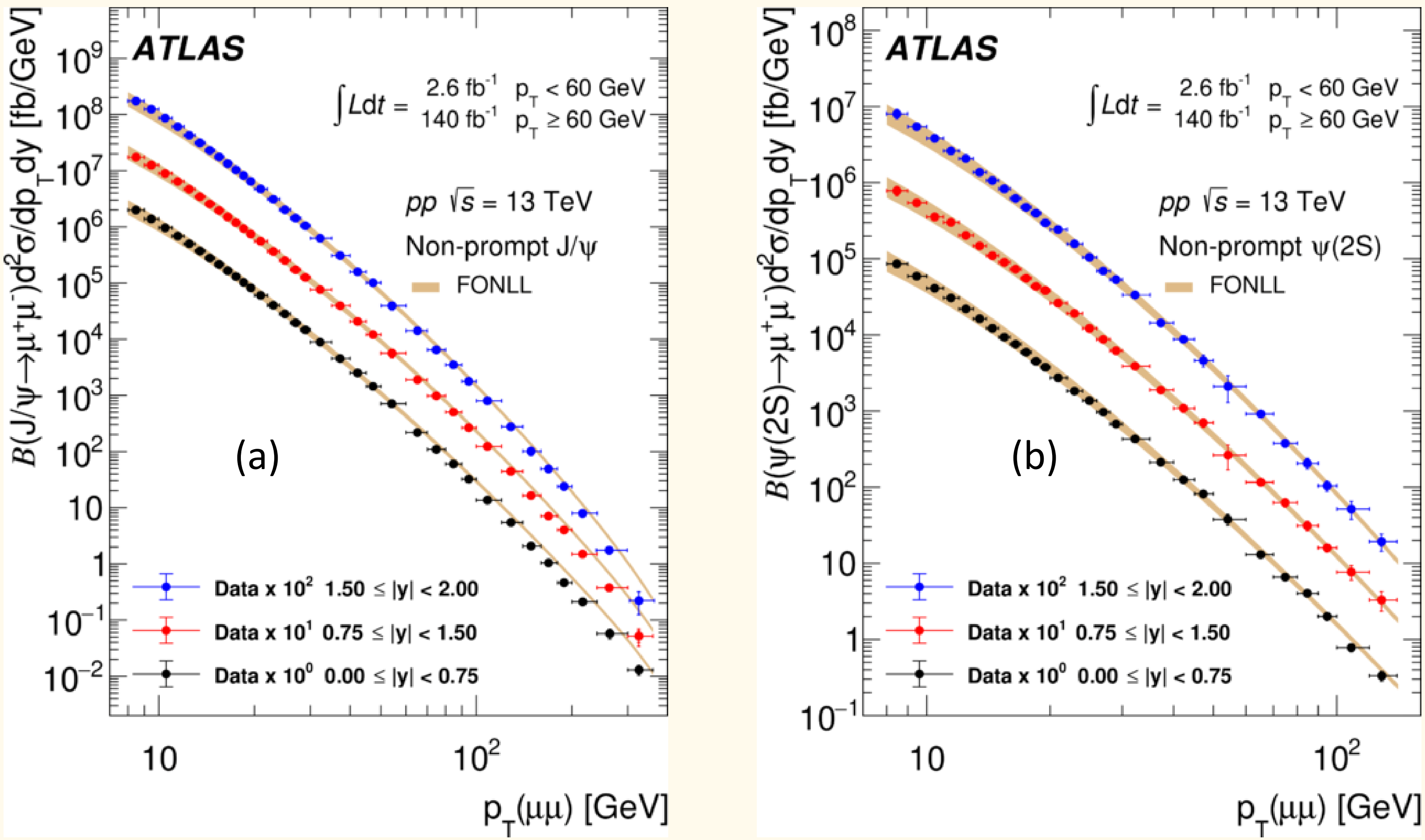

ATLAS arXiv:2309.17177 EPJC84(2024)169

The non-prompt differential cross-section overlaid with FONLL [9,10,11] predictions, shown for (a) J/ψ mesons, and (b) ψ(2S) mesons. The spread of the FONLL prediction band covers the effects of variation of hard scale and charm quark mass.

ATLAS data vs Kniehl et al.

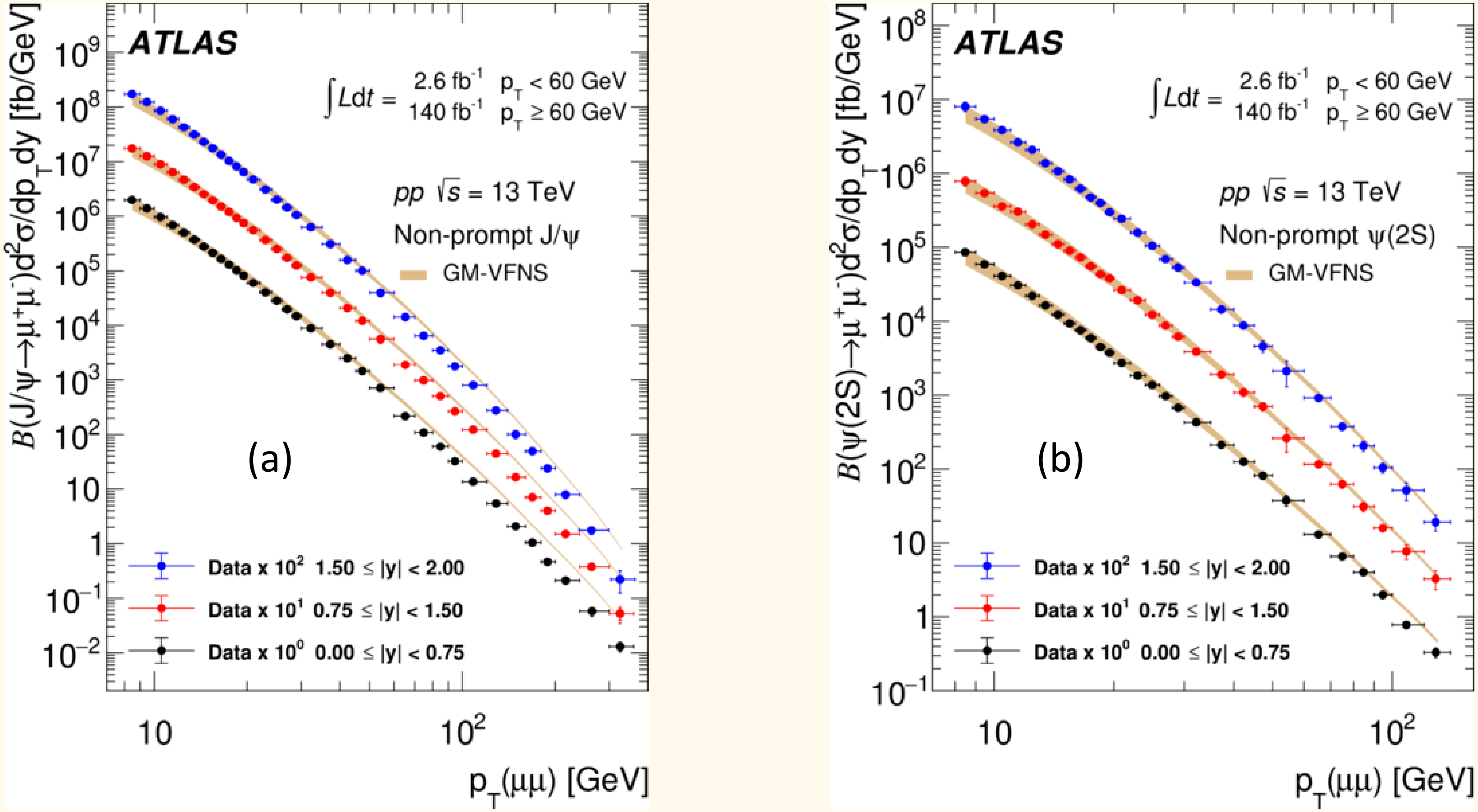

ATLAS arXiv:2309.17177 EPJC84(2024)169

Differential cross sections of non-prompt J/ψ (a) and non-prompt ψ(2S) (b) overlaid with predictions of the model based on the next-to-leading order QCD calculation in the general-mass-variable-flavor-number scheme (GM-VFNS) [12]. Parameters of the model were determined in Ref. [2,13], with uncertainties due to renormalisation scale dependence.

ATLAS data vs Baranov et al.

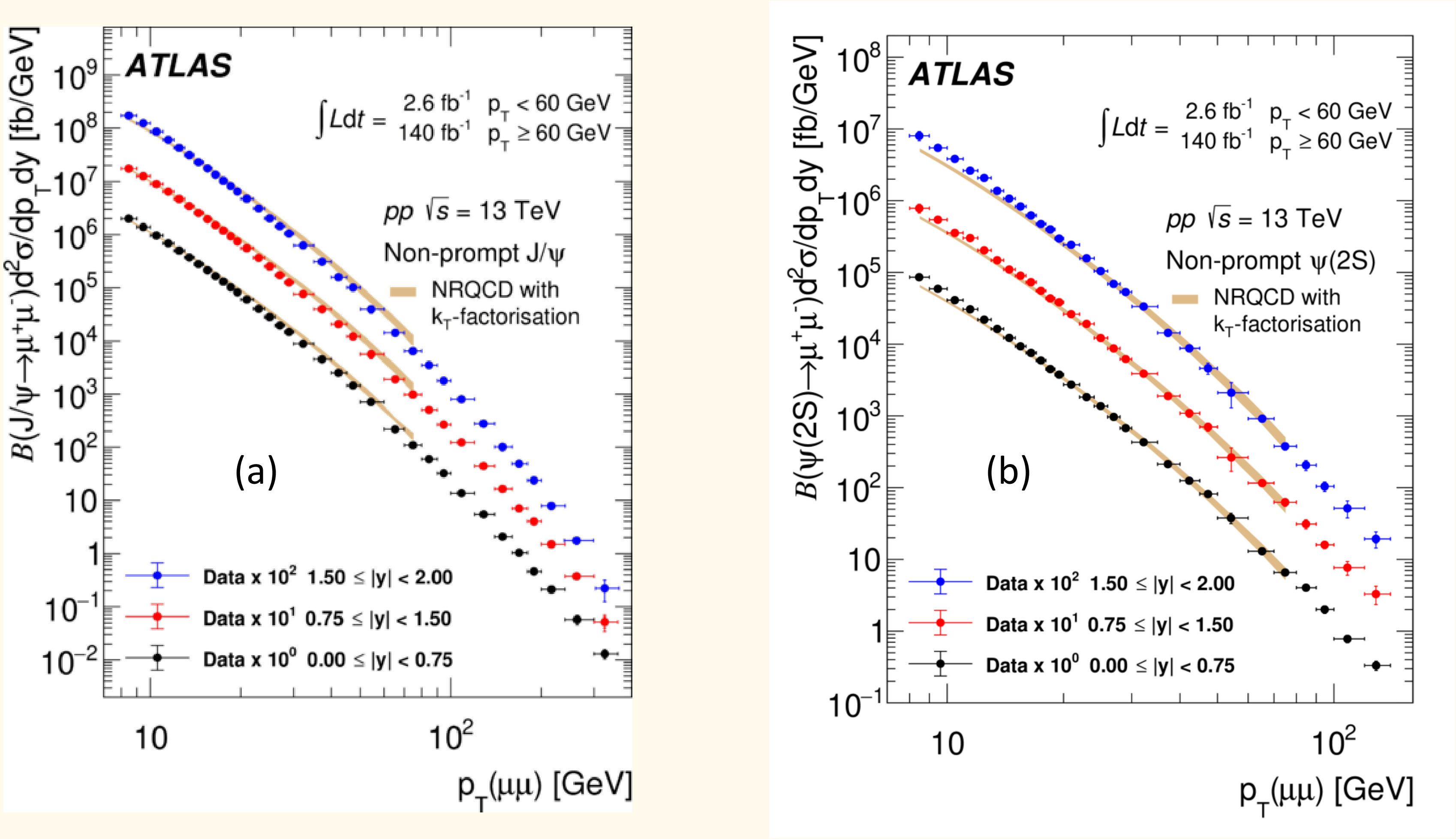

ATLAS arXiv:2309.17177 EPJC84(2024)169

Differential cross sections of non-prompt J/ψ (a) and non-prompt ψ(2S) (b) overlaid with predictions of the NRQCD model with k_T-factorisation [6,15]. The range of comparison is limited by the availability of the transverse-momentum-dependent gluon PDF.

The ATLAS detector at LHC